International Journal of Pharmaceutics 388 (2010) 263–273

Contents lists available at ScienceDirect

International Journal of Pharmaceutics

journal homepage: www.elsevier.com/locate/ijpharm

Pharmaceutical Nanotechnology

Effect of aqueous solubility of grafted moiety on the physicochemical properties of poly(D,L-lactide) (PLA) based nanoparticles

Sherief Essa, Jean Michel Rabanel, Patrice Hildgen*

C.P. 6128, succursale centre-ville, Montréal, Québec, Canada H3C 3J7

ARTICLE INFO

Article history:
Received 21 October 2009
Received in revised form
22 December 2009
Accepted 28 December 2009
Available online 8 January 2010

Keywords:
Poly(D,L-lactide)
PEG–PLA NPs
Palmitic acid-PLA NPs
Chain organization
X-ray photoelectron spectroscopy (XPS)
Phase imaging atomic force microscopy (AFM)

ABSTRACT

In order to evaluate the solubility effect of grafted moiety on the physicochemical properties of poly(D,L-lactide) (PLA) based nanoparticles (NPs), two materials of completely different aqueous solubility, polyethylene glycol (PEG) and palmitic acid were grafted on PLA backbone at nearly the same grafting density, 2.5% (mol of grafted moiety/mol of lactic acid monomer). Blank and ibuprofen-loaded NPs were fabricated from both polymers and their properties were compared to PLA homopolymer NPs as a control. NPs were analyzed for major physicochemical parameters such as encapsulation efficiency, size and size distribution, surface charge, thermal properties, surface chemistry, % poly(vinyl alcohol) (PVA) adsorbed at the surface of NPs, and drug release pattern. Encapsulation efficiency of ibuprofen was found to be nearly the same for both polymers ~36% and 39% for PEG2.5%-g-PLA and palmitic acid2.5%-g-PLA NPs, respectively. Lyophilized NPs of palmitic acid2.5%-g-PLA either blank or loaded showed larger hydrodynamic diameter (~180 nm) than PEG2.5%-g-PLA NPs (~135 nm). PEG2.5%-g-PLA NPs showed lower % of PVA adsorbed at their surface (~5%, w/w) than palmitic acid2.5%-g-PLA NPs (~10%, w/w). Surface charge of palmitic acid2.5%-g-PLA NPs seems to be influenced by the large amount of PVA remains associated within their matrix. Thermal analysis using DSC revealed possible drug crystallization inside NPs. Both AFM phase imaging and XPS studies revealed the tendency of PEG chains to migrate towards the surface of PEG2.5%-g-PLA NPs. While, XPS analysis of palmitic acid2.5%-g-PLA NPs showed the tendency of palmitate chains to position themselves into the inner core of the forming particle avoiding facing the aqueous phase during NPs preparation using O/W emulsion method. The in vitro release pattern showed that PEG2.5%-g-PLA NPs exhibited faster release rates than palmitic acid2.5%-g-PLA NPs. PEG and palmitate chains when grafted onto PLA backbone, different modes of chain organization during NPs formation were obtained, affecting the physicochemical properties of the obtained NPs. The obtained results suggest that the properties of PLA-based NPs can be tuned by judicious selection of both chemistry and solubility profile of grafted material over PLA backbone.

1. Introduction

Controlled release technology began in 1970s and since that time great interest has been paid to this technology. Recently, colloidal drug carriers are widely used for the development of controlled release systems for large number of drugs. Those carriers possess important applications in the pharmaceutical field. Moreover, they offer numerous advantages over conventional drug delivery systems such as controlled drug release rate, improved therapeutic efficiency, prolonged biological activity and decreased administration frequency (Letchford and Burt, 2007). They may also act as stabilizer protecting entrapped drugs against degradation. A way of modifying the original pharmacokinetics and biodistribution of drugs is to incorporate them in submicroscopic colloidal carriers. Numerous classes of colloidal carriers composed of different materials including lipids, polymers and inorganic materials have been developed, resulting in different delivery systems that vary in their physicochemical properties and thus their pharmaceutical uses. Growing interest in formulating NPs from synthetic polymers with tunable properties is rapidly expanding.

Despite the identification of various factors that might influence the properties of polymeric NPs such as the physicochemical properties of polymer and the drug (Frank et al., 2005), their interaction with each other (Jeong et al., 1998), drug load (Chorny et al., 2002), drug distribution inside the carrier, and size and morphology of the carrier (Gorner et al., 1999), chemical constitution effect and solubility profile of grafted moiety of the used polymer on various drug delivery aspects remains to be adequately addressed. Although different nanosystems have been developed, the effect of grafting the starting polymer with various grafted moieties needs to be realized

* Corresponding author. Tel.: +1 514 343 6448; fax: +1 514 343 6871.
E-mail address: Patrice.hildgen@umontreal.ca (P. Hildgen).

0378-5173/$ – see front matter © 2010 Elsevier B.V. All rights reserved.
doi:10.1016/j.ijpharm.2009.12.059

and emphasized for each nanosystem. In fact, grafting the same polymer with different materials will not only affect the physicochemical properties of the polymer, but also various drug delivery facets including, drug release rate, pharmacokinetics and biodistribution of the carrier, and even cellular uptake of the nanocarrier in vivo. It was previously shown that the molecular architecture of the polymer affects the cellular interaction of NPs prepared from different polymers (Sant et al., 2008).

This work is the first in-depth study of the effect of chain organization of the grafted moiety of the starting polymer on the major physicochemical aspects of drug delivery from PLA-based NPs, e.g. size of the carrier, surface charge, matrix erosion, and drug release profile. NPs formulated using PLA-b-PEG block copolymers were extensively investigated in the past (Govender et al., 2000; Heald et al., 2002; Vila et al., 2004). Up to now, however, relatively fewer studies have focused on grafted pegylated copolymer of PLA and PEG, used in our study.

Objective of the present work is to compare the effect of two grafted materials of different composition and aqueous solubility on the physicochemical properties of PLA-based NPs. Effect of grafted moiety on polymer chains organization during NPs formation was also investigated using relatively new techniques like XPS and phase imaging-AFM. PLA homopolymer was proposed as the control NPs and either hydrophilic (PEG) or hydrophobic (palmitic acid) substance was grafted onto PLA backbone at nearly the same grafting density 2.5% (mol/mol of lactic acid monomer), according to a previously published method by our group (Nadeau et al., 2005). Ibuprofen was used as a model lipophilic drug to be encapsulated by PLA and grafted PLA NPs. NPs were prepared using (O/W) emulsion-solvent evaporation method. PVA was used as an emulsifier during NPs preparation since it aids the formation of relatively small sized particles with uniform size distribution (Sahoo et al., 2002).

2. Materials and methods

2.1. Materials

D,L-Dilactide, poly(ethylene glycol) methyl ether (MePEG; 2000 Da), allyl glycidyl ether, tetraphenyltin, polyvinyl alcohol (PVA, average M_w 9000–10,000 Da, 80% hydrolyzed), pyridine, acetone, diethyl ether, thionyl chloride, borane-tetrahydrofuran complex (1 M), and palmitoyl chloride were purchased from Aldrich Chemical Company Inc., Milwaukee, USA. Ibuprofen was obtained from Medisca Pharmaceutical Inc., Montreal, Quebec, Canada. Sodium hydroxide pellets were purchased from Anachemia Canada Inc. and dichloromethane (DCM) was purchased from Laboratoire Mat Inc., Montreal, Quebec, Canada.

2.2. Synthesis of polymers

Poly(D,L)-lactide (PLA) was synthesized by ring-opening polymerization of dilactide in argon atmosphere, using tetraphenyltin as the catalyst. Briefly, dilactide was crystallized from toluene solution and dried under vacuum before use. A weighed amount of purified dilactide was then placed in a round-bottom flask and purged thoroughly with argon. Bulk polymerization was carried at 180 °C for 6 h. The polymer thus obtained was dissolved in acetone and was purified by precipitating in water.

Polymer with poly(ethylene glycol)-grafted randomly on poly(D,L)-lactide (PEG2.5%-g-PLA) (PEG; M_w 2000 Da) was synthesized in our laboratory as reported earlier (Nadeau et al., 2005). Briefly, D,L-dilactide (21.5 g, 97.5 mol%) was polymerized in the presence of allyl glycidyl ether (0.872 g, 2.5 mol%) with tetraphenyltin as the catalyst (1:10,000 mol with regards to D,L-dilactide) at 180 °C for 6 h under argon. Polylactic acid with allyl groups was purified by dissolving in acetone and precipitating in water. The allyl groups were converted to hydroxyl groups by hydroboration with an equimolar quantity of borane in tetrahydrofuran, followed by oxidation in the presence of hydrogen peroxide under alkaline conditions (1.5 mol of 3N sodium hydroxide). The hydroxyl groups were oxidized to carboxylic acid groups using Jones reagent, which was further converted to an acid chloride using thionyl chloride (1:1000 M). Finally, methoxy-PEG was grafted onto the polymer backbone by the reaction between acid chloride and the hydroxyl groups of methoxy-PEG (2000 Da) in the presence of pyridine. The final polymer was purified by evaporating pyridine and washing with distilled water.

Palmitic acid grafted on PLA backbone at 2.5% grafting density, palmitic acid2.5%-g-PLA was synthesized as follows, to a solution of PLA grafted with 2.5% hydroxyl pendant groups (1 g, 0.136 mmol) in 50 mL pyridine, palmitoyl chloride (1.8 g, 6 mmol) was added. The solution was stirred for 3 h and then, 10 mL water was added. The solvent was evaporated and the product was crystallized in diethyl ether to obtain a yellow product.^{1}H NMR spectra were recorded on a Brucker ARX 400 spectrometer (Bruker Biospin, Billerica, MA). Chemical shifts (δ) were measured in parts per million (ppm) using tetramethylsilane (TMS) as an internal reference. Gel permeation chromatography (GPC) was performed on a Water Associate chromatography system (Waters, Milford, MA) equipped with a refractive index detector and a Phenomenex Phenogel 5 μ column. Polystyrene standards were used for calibration with THF as the mobile phase at a flow rate of 0.6 mL/min.

2.3. Preparation of nanoparticles (NPs)

NPs were prepared using an (O/W) emulsion-solvent evaporation method. For blank NPs, each polymer (1 g) was dissolved in 35 mL DCM and emulsified in 100 mL PVA solution (0.5%, w/v) as an external aqueous phase using high-pressure homogenizer (Emulsiflex C30, Avestin, Ottawa, Canada) at a pressure of 10,000 psi for 5 min. The emulsion was collected by washing with another 100 mL 0.5% PVA. The DCM was evaporated under reduced pressure with constant stirring to obtain the NPs. Finally, NPs obtained as a suspension were then collected by centrifugation at 18,500 rpm for 1 h at 4 °C (Sorval® Evolution$_{RC}$, Kendro, USA), washed four times with distilled water, then lyophilized to obtain dry NPs (Freeze Dry System, Lyph.Lock 4.5, Labconco) and stored at 4 °C until further use. Ibuprofen-loaded NPs were prepared in a similar manner to that of blank NPs using initial loading of 10% (w/w) of each polymer. Ibuprofen was first dissolved in the organic phase followed by dissolution of the polymer. The emulsification and purification steps procedure were repeated as before.

2.4. Characterization of NPs

2.4.1. Particle size and zeta (ζ) potential measurements

The mean hydrodynamic diameters (d_h) and the polydispersity indices (PDIs) of NPs were measured by DLS with a Malvern Autosizer 4800 instrument (Malvern Instruments, Worcestershire, UK) before and after lyophilization. For all samples, fresh NP suspensions (0.1 mL) or lyophilized NPs (1 mg) were diluted 10 times with Milli-Q Water. Measurements were taken at a fixed scattering angle of 90° and at 25 °C. The CONTIN program was used to extract size distributions from the autocorrelation functions. Zeta-potential measurements of NPs suspended in 0.25% (w/v) saline solution (pH 7.4) were done on Malvern ZetaSizer Nanoseries ZS (Malvern Instruments, Worcestershire, UK). Both measurements were performed in triplicate

2.4.2. Determination of residual PVA

A colorimetric analysis was used for determination of PVA amount remaining in the NPs. The method is simply based on the formation of a colored complex between two adjacent hydroxyl groups of PVA and an iodine molecule (Sahoo et al., 2002). For surface associated PVA, certain weight of NPs was suspended in distilled water followed by vigorous vortexing for 10 min, then fixed volumes of all formulations were taken followed by addition of 5 mL of saturated solution of boric acid and 0.5 mL iodine (0.1N), and the volume was made up to 10 mL with distilled water. The absorbance of the formed complex was measured at 660 nm against similarly treated blank. Whereas for the total amount of PVA associated with the particles (amount entrapped inside the matrix as well as present on the surface), NPs were digested in 1N NaOH then neutralized by 1N HCl followed by stirring for 1 h and the volume was made up to 5 mL with distilled water. To this, 3 mL of saturated solution of boric acid and 0.5 mL iodine (0.1N) were added, and the volume was made up to 10 mL with distilled water. The absorbance was measured as before. PVA actual amount was calculated by using a calibration curve of PVA prepared under the same conditions.

2.4.3. NPs surface morphology and phase image analysis

Nanoscope IIIa Dimension 3100 atomic force microscope (Digital Instruments, Santa Barbara, CA, USA) was used to study both surface morphology and phase imaging of lyophilized NPs. Samples were prepared by deposition of particles suspension in Milli-Q Water on freshly cleaved mica followed by air-drying for 10 min at room temperature. Topography and phase images of these samples were captured simultaneously using TappingMode™ etched silicon probes (TESP7) with tip radius of 5–10 nm, spring constant of 20–100 N/m and resonance frequency of 200–500 kHz. Cantilever length was 125 μm.

2.4.4. Encapsulation efficiency (EE)

For ibuprofen-loaded NPs of PLA homopolymer and PEG2.5%-g-PLA, weighed amount of NPs was digested in 1N NaOH for 1 h. Ibuprofen concentration was measured by spectrophotometry at 264 nm (U-2001 UV/Visible spectrophotometer, Hitachi). While, for palmitic acid2.5%-g-PLA loaded NPs, weighed NPs were also suspended in 1N NaOH for 1 h to which chloroform was added followed by vigorous stirring for another 3 h to extract ibuprofen into the chloroform layer. Then, the chloroform layer was collected and ibuprofen concentration was measured by spectrophotometry at 263 nm. Percent encapsulation efficiency (% EE) and % actual loading efficiency (% LE) were calculated based on the following equations:

$$\%\,\mathrm{EE} = \frac{\text{Amount of drug entrapped in NPs}}{\text{Initial amount of drug added}} \times 100 \quad (1)$$

$$\%\,\mathrm{LE} = \frac{\text{Amount of drug entrapped in NPs}}{\text{Total amount of NPs}} \times 100 \quad (2)$$

2.4.5. Differential scanning calorimetry (DSC)

The thermal properties of polymers and drug in the physical mixture and NPs were characterized by DSC analysis (DSC 30, Mettler TA 4000, Schwerzenbach, Switzerland) with refrigerated cooling. Measurements were done ($n = 2$) on all investigated samples. Physical mixtures were prepared by triturating polymer and ibuprofen in a ratio similar to drug-loaded NPs. In brief, weighed samples were sealed in crimped aluminum pans with lids and heated at a rate of 10 °C/min from −50 to 200 °C for polymers and physical mixtures, while for NPs the samples were heated from −50 to 90 °C at the same heating rate.

2.4.6. XPS analysis

X-ray photoelectron spectroscopy, XPS (VG Scientific ESCALAB MK II) with a monochromatized Mg Ka X-rays ($h\nu$ 1253.6 eV) and an electron take off angle of 0° was used to study the surface chemistry of pure materials, polymers, blank, and drug-loaded NPs. A single survey scan spectrum (0–1000 eV) and narrow scans for C1s (210–305 eV) and O1s (525–550 eV) were recorded for each sample with a pass energy of 1 and 0.5 eV, respectively. Acquisition and data analysis were performed by a VGS 5000 data system. Peak fitting of the C1s envelope was as described by Shakesheff et al. (1997).

2.4.7. ^{1}H NMR spectroscopy

50 mg of lyophilized NPs of each polymer was suspended in deuterium Oxide (D_2O). ^{1}H NMR spectra were recorded on a Brucker ARX 400 spectrometer (Bruker Biospin, Billerica, MA). Chemical shifts (δ) were measured in parts per million (ppm) using tetramethylsilane (TMS) as an internal reference.

2.4.8. Erosion study

Mass losses of PLA (A), PEG2.5%-g-PLA (B), and palmitic acid2.5%-g-PLA (C) NPs were done by suspending 50 mg of NPs for each time interval in 10 mL PBS, pH 7.4 at 37 °C in shaking water bath. The study was terminated at 0, 5, 14, 25, 35 and 45 days. Samples were centrifuged (5000 rpm, 10 min) at the end of each time interval. The residues were washed two times with water to remove phosphate buffer and lyophilized for 24 h. The final mass of NPs was determined at each time point.

2.4.9. In vitro drug release study

NPs formulations prepared using different polymers were tested for in vitro release of ibuprofen in triplicates in phosphate buffered saline (PBS, 10 mM, pH 7.4). 150 mg NPs were suspended in 3.5 mL PBS in a dialysis tubing (Spectra Por 1 membrane, 6–8 kDa cut-off). This dialysis tubing was placed in a screw-capped tube containing 10 mL PBS. The tubes were shaken at 200 rpm on a horizontal water bath shaker (Orbit Shaker Bath, Labline) maintained at 37 ± 0.5 °C. At predetermined time intervals, the whole medium in the tube was withdrawn and replaced by fresh PBS to maintain sink conditions. The aliquots were assayed for the concentration of ibuprofen released by spectrophotometry at 262 nm.

3. Results and discussion

3.1. Characterization of polymers

Gel permeation chromatography (GPC) was used to measure molecular weight and molecular weight distribution of the synthesized polymers. Results are shown in Table 1. The polydispersity was calculated by the ratio of M_w to M_n from the GPC data. All the synthesized polymers exhibited uniform molecular weight distribution as revealed by the narrow polydispersity index values. Unimodal mass distribution ruled out the possibility of the presence of unreacted MePEG or palmitoyl chloride with poly(D,L-lactide). Typical spectrum was obtained for PLA homopolymer with a characteristic peak at 5.2 ppm corresponding to the tertiary PLA proton (m, –CH), and another peak at 1.5 ppm for the pendant methyl group of the PLA chain (m, $–CH_3$) (spectrum not shown). ^{1}H NMR spectra and chemical structures of PEG2.5%-g-PLA and palmitic acid2.5%-g-PLA polymers are shown in Fig. 1. A characteristic peak at 5.2 ppm corresponding to the tertiary PLA proton (m, –CH) was observed. Another characteristic peak at 3.6 ppm for the protons of the repeating units in the PEG chain (m, $OCH_2–CH_2O$), a peak at 4.3 ppm for the PEG connecting unit to the PLA block (m, $CH_2–OCO$), and a peak at 1.5 ppm for the pendant methyl group of the PLA chain (m, $–CH_3$) were also observed. The grafting density of PEG over the PLA backbone was calculated by comparing the peak

Table 1
Polymers characterization by ^{1}H NMR, DSC, and gel permeation chromatography (GPC).

Polymer	M_n[a]	M_w[a]	M_w/M_n[a]	PEG/palmitate (mol%)[b]	M_n (^{1}H NMR)[b]	T_g[c]
PLA	40,318	56,171	1.4	N/A	N/A	46.4 °C
PEG2.5%-g-PLA	4706	5171	1.1	2.3%	8209	50 °C
Palmitic acid2.5%-g-PLA	10,185	14,050	1.4	1.02%	14,514	19 °C

N/A: not analyzed.
[a] Determined by GPC analysis using narrow molecular weight polystyrene standards. M_w/M_n = polydispersity index of the polymers (PDI).
[b] Calculated from peak intensity ratios of PEG (3.6 ppm) in PEG2.5%-g-PLA or palmitate CH_3 (0.9 ppm) in palmitic acid2.5%-g-PLA and PLA (5.2 ppm) from ^{1}H NMR data analysis.
[c] Calculated from the second run of DSC as half of the extrapolated tangents in case of PLA and palmitic acid2.5%-g-PLA or as an endothermic peak in case of PEG2.5%-g-PLA.

intensity ratios of PEG (3.6 ppm) to that of PLA (5.2 ppm). The actual PEG grafting density was found to be 2.3% that is close to the initial feed ratio of PEG as shown in Table 1. For palmitic acid2.5%-g-PLA polymer, the signal observed at 1.2–1.3 ppm corresponds to the twelve hydrogens of the palmitate CH_2. The signal at 0.8–0.9 ppm is due to the palmitate CH_3. Palmitate grafting density was calculated by comparing peak intensity ratio of palmitate CH_3 (0.9 ppm) and PLA (5.2 ppm). The final palmitic acid grafting percentage was 1.02% that is also close to the initial feed ratio as shown in Table 1.

3.2. Particle size and size distribution

Dynamic light scattering (DLS) data showed unimodal distribution for freshly prepared and lyophilized NPs in all batches. Different blank formulations showed nearly similar particle size to that of loaded ones for all NPs types in the range of 120–200 nm (Table 2). This might indicate that drug loading had no observable effect on NPs size, suggesting that the size was mainly controlled by homogenization parameters during NPs preparation. Lyophilized palmitic acid2.5%-g-PLA NPs either blank or loaded seems to have larger hydrodynamic diameters than those obtained with PEG2.5%-g-PLA NPs as shown in Table 2. This could be explained by the fact that palmitic acid2.5%-g-PLA NPs is more hydrophobic compared to PEG2.5%-g-PLA NPs. The hydrophobic nature of the obtained particles might induce their aggregating tendency due to hydrophobic interactions. The aggregating tendency of palmitic acid2.5%-g-PLA NPs was confirmed later by AFM surface analysis (Fig. 2(c), left panel, T). While in PEG2.5%-g-PLA, the polymer architecture will allow PEG chains to migrate freely towards the surface of NPs during NPs preparation by O/W emulsion method. This would create a steric barrier reducing NPs aggregating tendency.

3.3. Zeta (ζ) potential measurements

PLA and palmitic acid2.5%-g-PLA blank NPs showed low zeta potential (close to zero) values than expected, −3.5 mV and −0.4 mV, respectively. This low ζ-potential for both NPs could be attributed to the effective adsorption of PVA on the surface of NPs as will be seen in the next section which could mask the surface charge of PLA and/or palmitic acid in case of PLA and palmitic acid2.5%-g-PLA NPs, respectively. ζ-Potential value of palmitic acid2.5%-g-PLA NPs were lower than PLA NPs and this might be due to higher

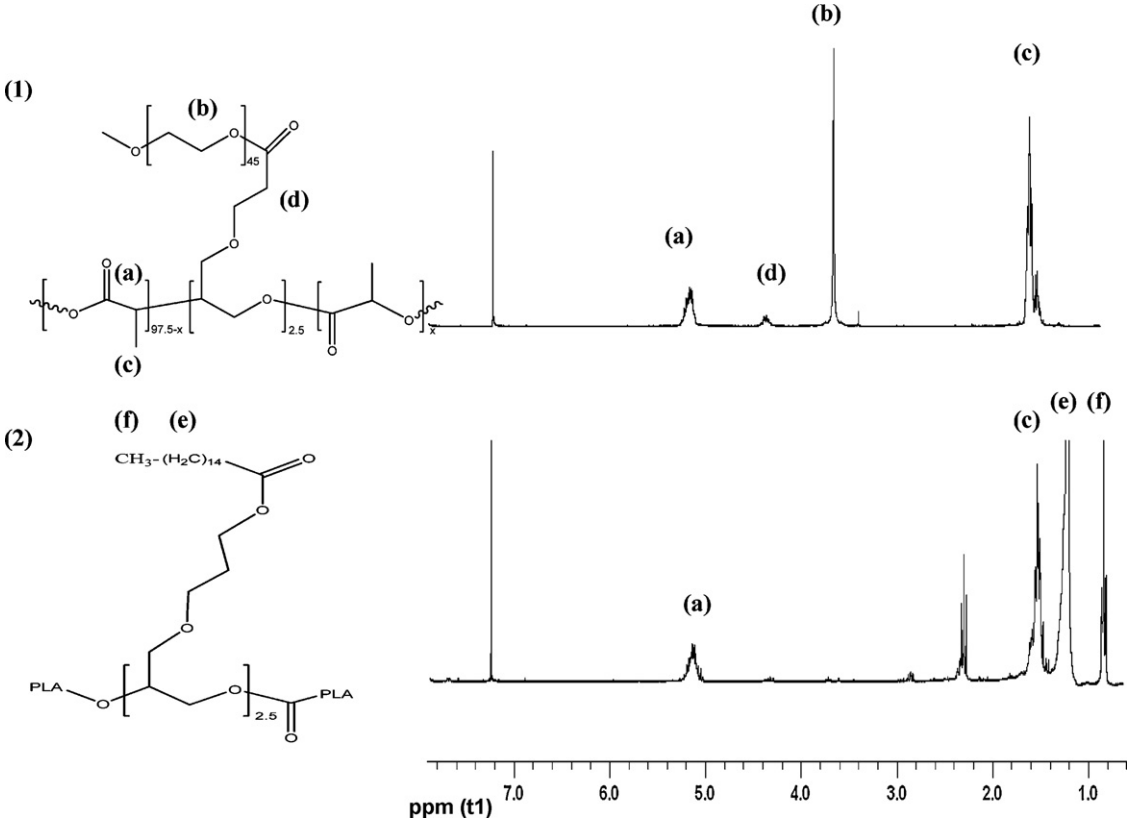

Fig. 1. ^{1}H NMR spectra and chemical structures of PEG2.5%-g-PLA (1), and palmitic acid2.5%-g-PLA (2).

Table 2
Characteristics of different NPs formulation.

Formulation	Size (d_h) before freeze drying (nm)[a,b]	PDI[c]	Size (d_h) after freeze drying (nm)[a,b]	PDI[c]	Actual loading (%, w/w)[b]	% EE[d,b]	Zeta potential (mV)[a,b]	Surface adsorbed PVA (%, w/w)[b]
PLA[e]	184 ± 20.8	0.13	161 ± 18.4	0.01	N/A	N/A	−3.50 ± 3.1	6.76 ± 0.4
PLA[f]	194 ± 30.0	0.08	162 ± 22.3	0.09	4.50 ± 0.2	45.0 ± 2.2	−0.18 ± 3.2	6.80 ± 0.2
PEG2.5%-g-PLA[e]	122 ± 31.6	0.14	145 ± 24.7	0.03	N/A	N/A	−1.30 ± 3.5	4.87 ± 0.4
PEG2.5%-g-PLA[f]	135 ± 22.9	0.11	135 ± 32.7	0.01	3.56 ± 0.1	36.6 ± 1.5	−0.60 ± 3.9	5.00 ± 0.7
Palmitic acid2.5%-g-PLA[e]	176 ± 19.7	0.04	181 ± 30.8	0.13	N/A	N/A	−0.40 ± 3.1	8.60 ± 0.4
Palmitic acid2.5%-g-PLA[f]	147 ± 22.4	0.06	183 ± 22.2	0.12	3.86 ± 0.2	39.5 ± 0.7	−0.14 ± 3.7	9.80 ± 0.5

N/A: not analyzed.
[a] Median.
[b] All values indicate mean ± S.D. for $n = 3$ independent measurements.
[c] Refers to polydispersity index.
[d] Refers to encapsulation efficiency.
[e] Refers to blank NPs (unloaded).
[f] Refers to loaded NPs.

amount of PVA adsorbed onto the surface (8.6%, w/w) compared to PLA NPs (6.7%, w/w) (Table 2). Loaded NPs of both polymers also showed low zeta potential values explained by the same reason. Zambaux et al. also obtained a low zeta potential value of −4 mV for PLA NPs prepared with PVA as an emulsifier (Zambaux et al., 1998). PEG2.5%-g-PLA NPs had also low zeta potential and this could be attributed to shielding action of PEG on the surface charge. Similar results to ours were reported earlier by other authors (Gref et al., 2000; Beletsi et al., 2005; Quesnel and Hildgen, 2005). Moreover, the greater reduction in zeta potential value of PEG2.5%-g-PLA NPs compared to other PEG–PLA NPs reported in the last cited references could be explained by the existence of PVA at the surface of NPs which played also a role in masking their actual surface charge. PEG2.5%-g-PLA NPs showed a remarkable adsorption of 5% (w/w) PVA onto their surface as shown in Table 2.

3.4. Residual PVA

One of the drawbacks of NPs formulation using emulsion-solvent evaporation method is the residual surfactant remaining in NPs suspension after particles precipitation in the aqueous phase. Residual surfactant becomes adsorbed onto the surface of freeze dried nanoparticles irrespective of the number of washing steps performed to remove it. This might lead to alteration of NPs physicochemical properties such as particle size, hydrophilicity, release kinetics, cellular uptake, etc. (Sahoo et al., 2002). PVA amount remained attached to the nanoparticles needed to be evaluated to detect whether they are affected by the composition and the architecture of the starting polymer or not. It could be seen that a different amount of PVA remained in all the formulations even after 4 washings (Table 2). It was found that the highest amounts of PVA remained attached to NPs matrix were 9.8% and 6.8% (w/w) for palmitic acid2.5%-g-PLA and PLA NPs, respectively (Table 2). This might be attributed to the enhanced hydrophobic interaction between acetate group of PVA and the hydrophobic PLA matrix as reported before by other authors (Scholes et al., 1999; Sahoo et al., 2002). Similar findings were obtained before by other authors. When 1% (w/v) PVA was used as an external aqueous phase emulsifier, 5–6% (w/w) PVA remained attached within PLA NPs even after 3 washings (Zambaux et al., 1998). PLGA NPs also exhibited a remarkable adsorption of 6.15% (w/w) PVA into their matrix when 5% (w/v) PVA solution was used as an emulsifier. Since palmitic acid2.5%-g-PLA is expected to be more hydrophobic than PLA so more interaction with acetate group of PVA might take place. PEG2.5%-g-PLA exhibited less PVA adsorption (5%, w/w, Table 2) onto their surface and this might be due to their PEG content which offered a certain degree of hydrophilicity to the NPs matrix so a less favored interaction with PVA should be expected. PVA amount adsorbed at the surface of more hydrophilic PLGA microspheres was found to be less than PLGA microspheres (Shakesheff et al., 1997). Also, blank NPs showed similar amount of PVA adsorbed on their surfaces as loaded NPs indicating that drug loading had no apparent effect on the amount of PVA associated within the NPs matrix. An attempt was made to evaluate whether PVA was present either inside the polymeric matrix or on the surface of the particles. Nearly the same amount of PVA was present in the given NPs for-

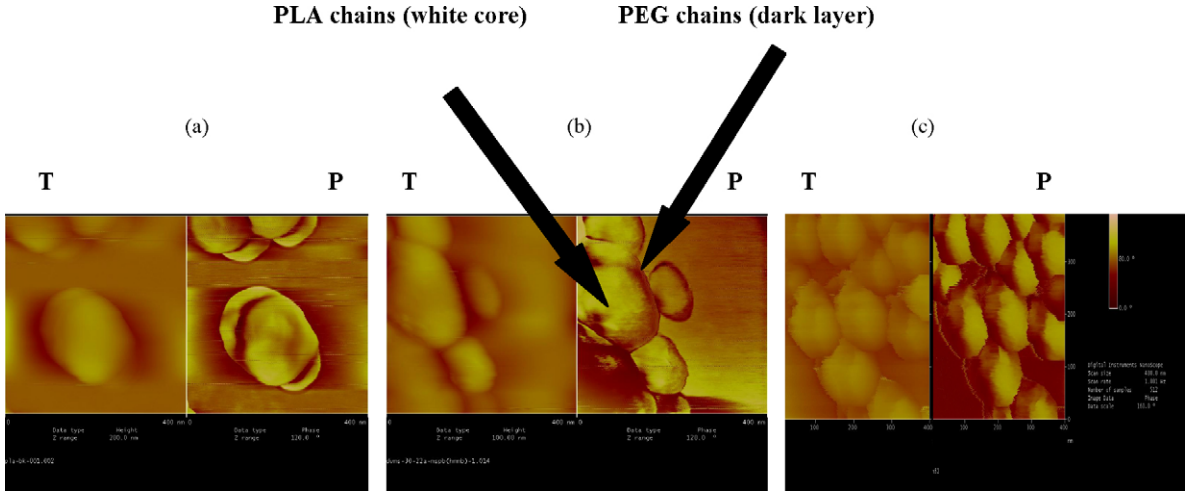

Fig. 2. Tapping mode AFM images of NPs, left panel shows topography (T) and right panel shows corresponding phase images (P); all images are acquired in air. Scan size [400 nm × 400 nm]; PLA (a), PEG2.5%-g-PLA (b), palmitic acid2.5%-g-PLA (c).

mulations by both assays confirming that the amount of PVA was mainly associated with the surface of the particles (data not shown).

3.5. Surface morphology and phase analysis

Tapping mode atomic force microscopy (TM-AFM) was used for analysis of surface morphology of NPs. TM-AFM revealed that both PLA and PEG2.5%-g-PLA NPs were spherical with smooth surfaces. While palmitic acid2.5%-g-PLA NPs seems to have some irregularities at their surface. This might indicated their aggregating tendency (Fig. 2(c), left panel, T) confirming the size data obtained by DLS. Phase image analysis was done to investigate the surface chemistry of the obtained particles. It shows more sensitivity to material surface properties such as stiffness, viscoelasticity, and chemical composition (Magonov et al., 1997; Raghavan et al., 2000; Paredes et al., 2005). Phase imaging is based on the use of changes in the phase angle of cantilever probe. Fig. 2 shows TM-AFM topography (left panel, T) and their corresponding phase images (right panel, P) of PLA, PEG2.5%-g-PLA, and palmitic acid2.5%-g-PLA NPs, respectively. It is evident from Fig. 2 that phase images displayed more contrast than the respective topographic images. Phase images of PLA NPs did not show any clear phase separation evidenced by no color contrast was observed [Fig. 2(a); right panel, P]. On the other hand, PEG2.5%-g-PLA NPs showed the presence of an observable phase contrast at the surface of NPs revealed by some dark layers at the surface of bright cores [Fig. 2(b); right panels, P]. PEG molecules of lower M_w 2000 (used in our study) have smaller Young's modulus than PLA so they are expected to be softer than PLA (Donald et al., 2003). Those mechanical differences between PLA and PEG will result in such phase contrast. Thus, it was expected that PEG molecule will result into darker regions for PEG in the phase images. This was investigated before for poly(styrene-b-ethylene oxide) polymer films, where softer PEG segments appeared as darker regions embedded in lighter polystyrene domain (Wang et al., 2005). The immiscibility of both PEG and PLA blocks would result in separation of both components during NPs formation. Thus, PEG2.5%-g-PLA NPs will be predominantly consisting of hydrophobic PLA cores surrounded by hydrophilic PEG chains on the surface (Fig. 2(b), phase image, P). While, in case of palmitic acid2.5%-g-PLA (Fig. 2(c)), NPs appear as if they were collapsed together with some deformation. This might be due to energy dissipation during tip-sample interaction. The last finding could be explained on the basis of the soft nature of the polymer resulted from grafting palmitic acid over PLA backbone. Palmitate chains are expected to lower the chain rigidity of PLA domains evidenced by the lower T_g of the polymer (19 °C) compared to PLA homopolymer (46.4 °C) as will be revealed from DSC data (Table 1). Another predisposing factor for palmitic acid-g-PLA NPs deformation by AFM tip is that they were dried at room temperature above their T_g (19 °C). This might favored the existence of the polymer chains in their mobile rubbery state.

3.6. Encapsulation efficiency (EE)

As seen from Table 2, % EE of ibuprofen was found to be 36.6% and 39.5% for PEG2.5%-g-PLA, and palmitic acid2.5%-g-PLA NPs, respectively. No marked difference between both polymers ability to encapsulate the drug was detected. This might be due to small grafting density of each polymer since 2.5% (mol of grafted subs./mol of lactic acid) might not be big enough to affect the loading level of PLA NPs. Another possible reason is the larger surface area of the obtained NPs that resulted from the smaller particle size of either PEG2.5%-g-PLA (135 nm) or palmitic acid2.5%-g-PLA NPs (147 nm), readily result in higher drug diffusion to the aqueous phase and hence, limited drug loading (Table 2) (Mohanraj and Chen, 2007). Moreover, grafting palmitate over PLA backbone might decreased the density of the obtained NPs (evidenced by low M_w of palmitic acid2.5%-g-PLA compared to high M_w PLA, Table 1) leading to slower precipitation of NPs compared to the denser PLA and this might give a chance for the drug to diffuse freely into the aqueous phase.

3.7. DSC

DSC was used to detect the effect of grafted substance of the used polymer on the thermal properties of NPs. DSC was also used for investigating any possible interaction between the drug and the polymeric matrix. PLA showed glass transition (T_g) at 46.4 °C (Table 2). Random grafting of PEG on the PLA backbone resulted in an increased T_g value (by about 4 °C) due to enhanced chain rigidity (Table 1 and Fig. 3(a)). For palmitic acid2.5%-g-PLA, the glass transition of the polymer was found to be 19 °C with the existence of an endothermic peak at 58 °C corresponding to the melting peak of the palmitic acid crystals (Table 2 and Fig. 3(b)). The melting endotherm of palmitic acid was shifted by 4 °C lower compared to pure palmitic acid indicating the possibility of physical interaction (hydrophobic interaction) between the grafted palmitic acid group and PLA. Also, this might indicate that some of palmitate chains are embedded inside PLA domain lowering its chain rigidity evidenced by the lower T_g of the polymer (19 °C) compared to PLA homopolymer (46.4 °C). Fatty acid esters were found to have a remarkable plasticizing actions on PLA chains (Jacobsen and Fritz, 1999). Ibuprofen showed an endothermic peak at 78 °C corresponding to the melting of ibuprofen crystals (Fig. 3(a)). As shown in Fig. 3(a), DSC curve of PEG2.5%-g-PLA/ibuprofen physical mixture showed an endothermic peak corresponding to the glass transition (T_g) at ~50 °C. The melting endotherm of ibuprofen crystals could also be detected at 74 °C. The drug melting peak was shifted by 4 °C lower with some broadening of the peak, indicating the possibility of an interaction between drug and polymer. After encapsulation of ibuprofen in the NPs, T_g was found to be reduced by 15 °C lower (~35 °C) and this due to the effect of formulation parameters. Surprisingly, the melting endotherm of ibuprofen crystals could also be detected at 74 °C with some broadening (Fig. 3(a)). For more verification, lyophilized loaded NPs were washed five times with water then centrifuged to remove the surface associated drug followed by their lyophilization. DSC scans were done again, surprisingly; the melting endotherrm of ibuprofen still exists. This might indicate the detected melting endotherrm is for encapsulated ibuprofen which was dispersed in a crystalline form (solid dispersion) not molecular dispersion into PLA matrix. Moreover, the shift and broadening of the melting peak also indicated that an interaction between the drug in its crystalline state and the polymer might take place. Similar observations were noticed with PLA (DSC figure not shown), and palmitic acid2.5%-g-PLA (Fig. 3(b)) in both physical mixtures and NPs with the consideration of different T_g for each investigated polymer. Similar finding to ours was obtained when lidocaine was embedded into PEG-PLGA nanospheres. Lidocaine exhibited an endothermic peak at lower temperature or broadened melting peak compared to lidocaine alone. The authors also suggested that there is an interaction between lidocaine and the polymeric carrier (Peracchia et al., 1997).

3.8. XPS analysis

Surface chemistry analysis of NPs prepared from both polymers was investigated by means of X-ray photoelectron spectroscopy (XPS) technique. It is possible to determine the surface chemical composition at a depth in the range of 1–10 nm. Any possible interaction between PLA and PVA at the surface of NPs could also be detected in that range. PVA polymer showed three main characteristic peaks corresponding to C–C/C–H (285 eV), C–OH (286.7 eV)

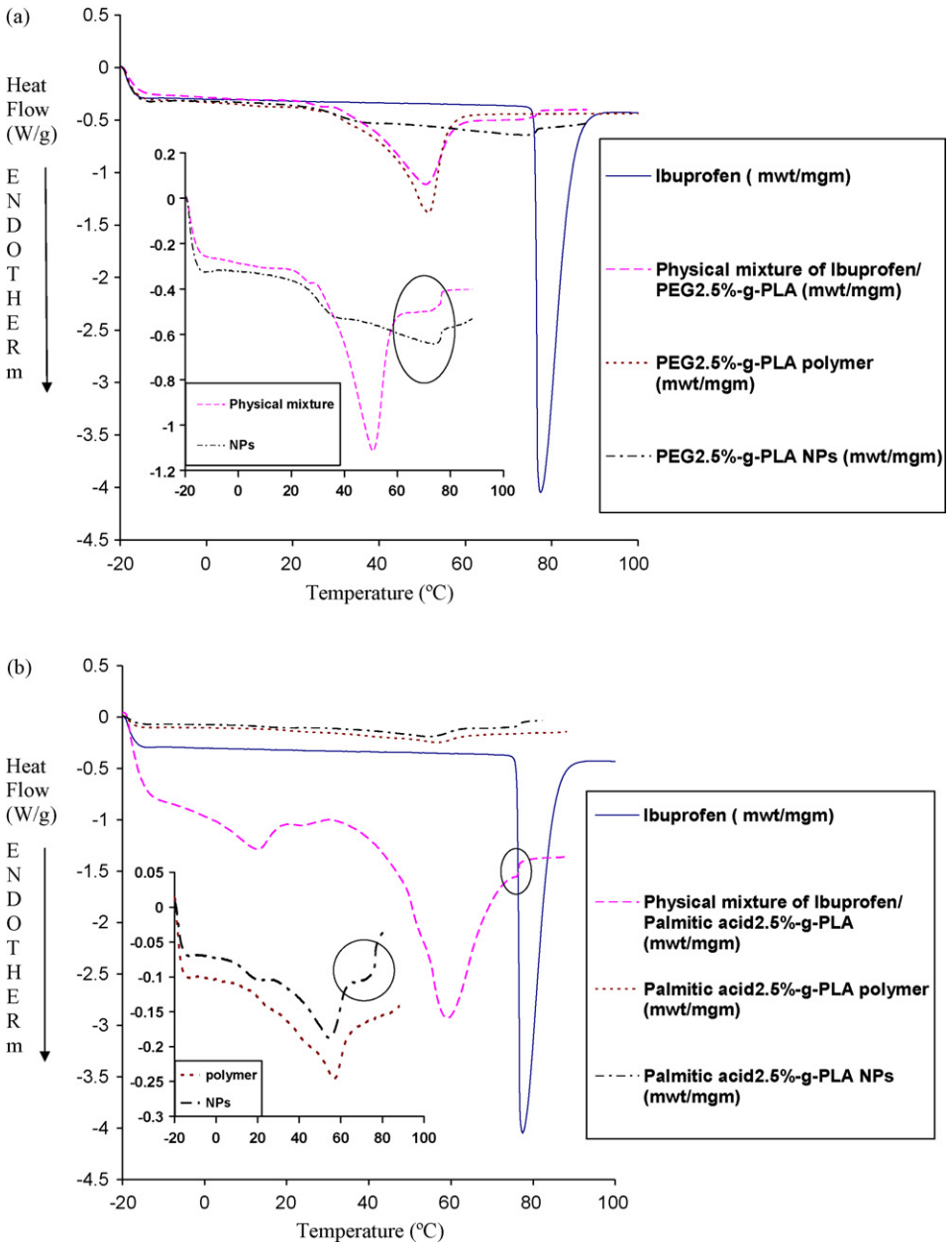

Fig. 3. (a) DSC curves of ibuprofen, physical mixture of PEG2.5%-g-PLA with ibuprofen, PEG2.5%-g-PLA polymer, and ibuprofen-loaded NPs. Inset inside the figure shows clear thermograms for both physical mixtures and NPs, ibuprofen melting peak is encircled. (b) DSC curves of ibuprofen, physical mixture of palmitic acid2.5%-g-PLA with ibuprofen, palmitic acid2.5%-g-PLA polymer, and ibuprofen-loaded NPs. Inset inside the figure shows clear thermograms for both pure polymer and NPs. Ibuprofen melting peak is encircled.

and O–C=O (289 eV) components (Table 3). XPS spectrum of PEG showed one characteristic peak corresponding to ether carbons (286.5 eV, Table 3). For PLA homopolymer, the best envelop fit was obtained using three main peaks corresponding to C–C/C–H (285 eV), C–OH (287 eV) and O–C=O (289 eV) (Table 3) as previously reported (Shakesheff et al., 1997). Ibuprofen could not be experimentally analyzed because it sublimes under the high vacuum of the equipment. Theoretically, ibuprofen has two main characteris-

Table 3
Relative atomic percentages calculated from XPS surface analysis of pure materials used in NPs preparation.

Binding energy (functional component)	Atomic percentage (%)			
	Ibuprofen	PLA	PVA	PEG
285 (C–C)	92.4	22.3	37.1	–
286.5 (C–O)	–	–	–	100
286.7 (C–O)	–	–	23	–
287 (C–O)	–	28.9	–	–
289 (O–C=O)	7.6	13.9	4.3	–

N.B: relative percentage of each functional component is calculated from the area under the curve from their respective peaks in XPS analysis.

Table 4
Relative atomic percentages calculated from XPS surface analysis of synthesized polymers and formulated NPs using those polymers.

B.E. (functional component)	Atomic percentage (%)					
	PEG2.5%-g-PLA BK NPs	PEG2.5%-g-PLA LD NPs	PEG2.5%-g-PLA polymer	Palmitate 2.5%-g-PLA BK NPs	Palmitate 2.5%-g-PLA LD NPs	Palmitate 2.5%-g-PLA polymer
285 (C–C)	7.3	10.8	10.0	49.1	42.8	63.8
286.2 (*C–O–C=O)	2.1	2.5	–	8.6	13.9	–
286.5 (C–O)	5.4	5.0	9.5	–	–	–
287.6 (C–O–*C=O)	4.2	3.5	–	5.3	5.0	–
289 (O–C=O)	5.5	4.1	5.0	5.7	2.2	4.6

(B.E.) refers to the binding energy; (BK) refers to blank NPs; (LD) refers to loaded NPs.

tic peaks corresponding to C–C/C–H (285 eV), and O–C=O (289 eV) components (Table 3). It should be mentioned that for ibuprofen to be detected at the surface of loaded NPs, an increase in atomic percentages of both its characteristic peaks mainly C–C/C–H (285 eV) is expected to be found. Both ibuprofen-loaded and blank NPs of PEG2.5%-g-PLA grafted polymer as well as the polymer itself showed the existence of PEG chains on the surface as seen by the presence of a characteristic peak corresponding to ether carbons (286.5 eV, Table 4). However, the atomic % of PEG decreased when the polymer (9.5%) was formulated into NPs either blank (5.4%) or loaded NPs (5%) as shown in Table 4. This might be due to surface adsorption of PVA in case of blank NPs as shown before in PVA analysis section. While in loaded NPs, both PVA and ibuprofen might be adsorbed at the surface of NPs as evidenced from the increase in atomic % of C–C (285 eV) in case of loaded NPs (10.8%) compared to blank NPs (7.3%) [Table 4]. Such an adsorption might decreases the PEG content at the surface. Also, it could be seen from Table 4 that the atomic % of C–C (285 eV) decreases from the polymer (10%) to blank (7.3%) and then increased again in case of loaded NPs (10.8%). This might be due to presence of more PLA chains collapsed inside the NPs core (oil phase) during NPs chain organization by O/W emulsion method with less existence of PLA and hence, the C–C functional component at the NPs surface. This C–C content lowering was compensated by drug adsorption (rich in C–C component) at the surface in case of loaded NPs. Moreover, to get the best envelop fit of both NPs, two additional peaks had to be added corresponding to C–O–*C=O (287.6 eV) and *C–O–C=O (286.2 eV) components (Table 4). These new peaks obtained in both types of NPs could be the result of chemical interaction between PLA–COOH end and PVA–OH during NP formation. The last finding also supports the effective masking of negative charge of these NPs by both PEG and PVA chains at the surface of such NPs as shown in Table 2. It was shown before that despite of several washing steps of the separated NPs pellets, there is always a fraction of PVA remains associated with the NPs and this has been attributed to the hydrophobic interactions between vinyl acetate segment of PVA and PLA/PLGA core (Sahoo et al., 2002). O–C=O functional component (289 eV) was detected also in the XPS spectrum of the PEG2.5%-g-PLA polymer, both its blank and loaded NPs. This might be due to the presence of COOH functional group in the polymer structure (Fig. 1) or due to adsorption of PVA (partially hydrolyzed) and ibuprofen (weak acid) at the surface of blank and loaded NPs, respectively. In case of palmitic acid2.5%-g-PLA polymer and its both NPs types, there was a marked decrease in C–C components (285 eV) atomic % from the polymer (63.8%) to blank (49.1%) and then to loaded NPs (42.8%). This might be due to chain organization during NPs formation by O/W emulsion method in such a way that showed the migration of palmitate (hydrophobic chain) towards NPs core (oil phase) to avoid facing the external aqueous phase. This process might force palmitate chains to be embedded into NPs core and hence decreasing the C–C content at the surface. Although we expected an increase in the atomic % of C–C (285 eV) from blank to loaded NPs as shown before with PEG2.5%-g-PLA loaded NPs, a decrease in the atomic % (from 49.1% to 42.8%) of that component was surprisingly detected and this might be to due to the possibility of hydrophobic interaction between ibuprofen and palmitic acid which forces the drug to be embedded inside the core of NPs. The last hypothesis was supported by another finding that the atomic % of O–C=O (289 eV) [also characteristic for the drug] was very low (2.2%) in case of loaded NPs (Table 4). This indicates that some interaction might occur between the drug and polymer shielding the drug functional groups from the surface. It also should be mentioned that the existence of that functional gp, O–C=O (289 eV) in the polymer and blank NPs spectra (4.6% and 5.7%, respectively) might be due to COOH of both PLA and PVA (partially hydrolyzed), respectively. Also, the existence of two new peaks at C–O–*C=O (287.6 eV) and *C–O–C=O (286.2 eV) might confirmed PVA interaction with PLA in such kind of polymer. This finding was also supported by the high % residual PVA detected at the NPs surface as shown in Table 2.

3.9. ^1H NMR of NPs in D_2O

^1H NMR analysis of NPs in D_2O was done to confirm the core–corona structure of PEG2.5%-g-PLA NPs and compare it with palmitate2.5%-g-PLA NPs structure. ^1H NMR spectra of PEG2.5%-g-PLA NPs in D_2O showed presence of methylene protons of PEG chains at 3.6 ppm (Fig. 4). Signals from PLA methyl or methylene protons were absent or diminished in intensity. Also both signals corresponding to the twelve hydrogens of the palmitate CH_2 and the palmitate CH_3 were completely absent in ^1H NMR spectra of palmitic acid2.5%-g-PLA. This might indicate that both PLA and

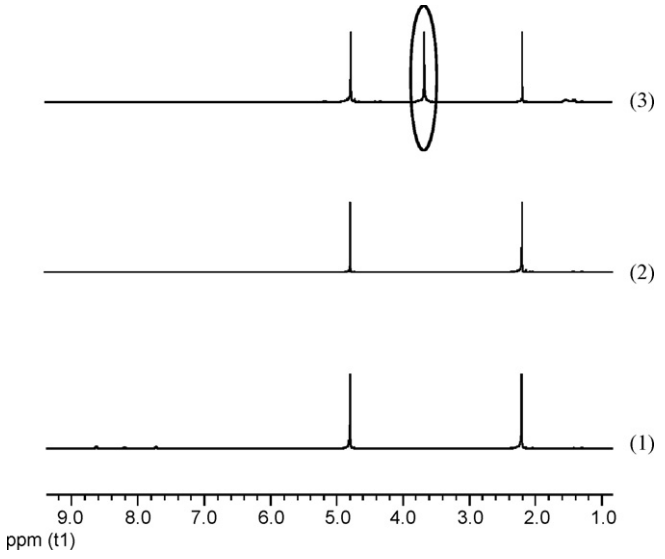

Fig. 4. ^1H NMR of blank NPs of PLA (1), palmitic acid2.5%g-PLA (2), and PEG2.5%g-PLA (3) in D_2O. PEG peaks at 3.6 ppm are encircled.

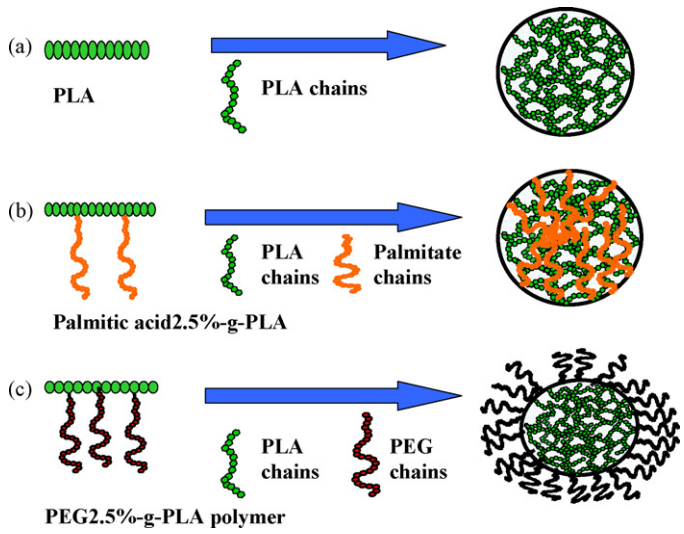

Fig. 5. Schematic representation of polymer chain organization inside the NPs: PLA (a), palmitic acid2.5%-g-PLA (b), PEG2.5%-g-PLA (c).

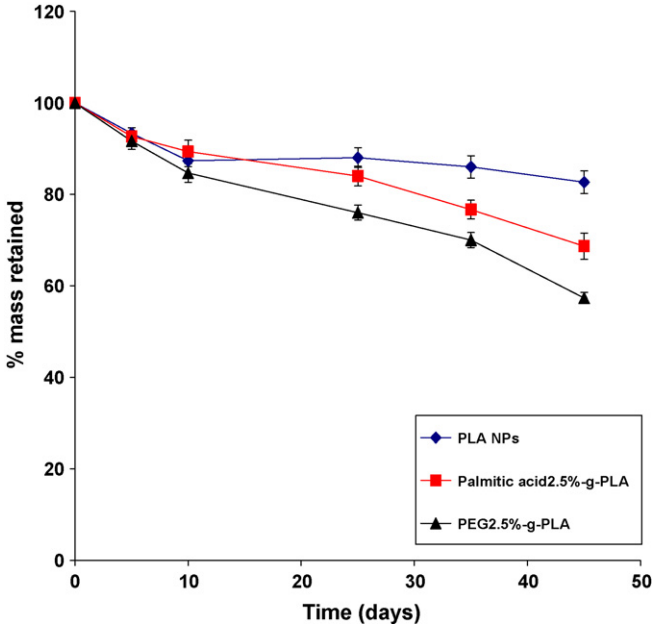

Fig. 6. Erosion of different ibuprofen-loaded NPs in phosphate buffer saline (PBS, pH 7.4) at 37 °C.

palmitate protons are in solid environment and cannot be detected whereas PEG chains must be in mobile state. Core–corona structure of PLA–PEG diblock NPs was confirmed before from ^{1}H NMR analysis of NPs in D_2O (Riley et al., 2001). ^{1}H NMR analysis was also used to confirm poly-(ethylene glycol)-b-(styrene-*r*-benzocyclobutene) block copolymer PEG-b-(S-*r*-BCB) NPs formation after intramolecular cross-linking of the S-*r*-BCB block to form a linear-nanoparticle structure. ^{1}H NMR spectra of NPs showed complete disappearance of the aliphatic benzocylobutene protons at 3.05 ppm upon formation of the cross-linked nanoparticles (Kim et al., 2005). Our results are in accordance with the above-cited references suggesting NPs made of PLA and PEG corona in case of PEG2.5%-g-PLA NPs. Thus, ^{1}H NMR analysis together with XPS data of NPs might indicate that hydrophilic polymer parts (PEG) are oriented towards the outer phase (water) during precipitation and NP hardening whereas the more lipophilic polyester (either PLA or PLA and palmitate) residues form the inner core. A schematic representation of different chain organization of NPs depending on both their polymer composition and polymer architecture is shown in Fig. 5. For PEG2.5%-g-PLA NP, enhanced phase separation of both components during NPs formation was observed as confirmed from AFM phase imaging, XPS and ^{1}H NMR data. Thus, easy migration of PEG chains towards the surface of NPs will be favored while the cores will be predominantly hydrophobic. On the contrary, palmitic acid2.5%-g-PLA NPs showed the migration of palmitate chains into PLA core avoiding facing the aqueous phase during NPs preparation.

3.10. Erosion study

This study was conducted to investigate the effect of polymer grafting on the in vitro degradation rate of PLA-based NPs under conditions similar to physiological ones. Mass loss of copolymer in phosphate buffer started after 5 days for all the investigated NPs. A noticeable difference in mass loss is observed between PEG2.5%-g-PLA and palmitic acid2.5%-g-PLA NPs after 10 days of incubation. PEG2.5%-g-PLA exhibited faster erosion rate ~43% compared to both PLA and palmitic acid2.5%-g-PLA NPs which showed slower rates around 17% and 32%, respectively after 45 days. This pattern is shown in Fig. 6. Mass loss of polyester copolymers is usually enhanced by ester hydrolysis and transesterification mechanisms (von Burkersroda et al., 1997). NPs erosion was initiated by water uptake followed by random hydrolytic chain scission of PLA block with release of lactide oligomers. The more hydrophilic PEG2.5%-g-PLA initially swells to a much greater degree than other polymers of lower hydrophilic content, allowing more water uptake into the matrix, further increasing the rate of hydrolysis and breakdown of NPs (Siparsky et al., 1997; Clapper et al., 2007). Thus PEG grafting over PLA backbone was observed to increase the degradation rate of PLA. The possible reason that palmitic acid2.5%-g-PLA NPs showed faster degradation rates than PLA NPs is that palmitic acid2.5%-g-PLA polymer has lower M_w compared to PLA homopolymer (Table 1).

3.11. In vitro drug release

One of the main purposes of this study is to compare and study the effect of the aqueous solubility of grafted substance over PLA backbone on drug release profiles from modified PLA NPs. Ibuprofen showed much more rapid release from solution than its release from the NPs indicating that drug diffusion through the dialysis bag was not the release rate-limiting step (Fig. 7). Different NPs formulations were compared for their in vitro release behavior as shown in Fig. 7. It could be seen that all formulations exhibited biphasic release phenomenon. A rapid initial burst release varied from 10% to 20% of their payload and this might be due to the immediate release of drug particles adsorbed at or near the surface of NPs (Magenheim et al., 1993). This phase was followed by sustained release of the drug over 300 h. Drug release during that phase is mainly controlled by solubility of the drug in the matrix, diffusion of drug into the matrix, and matrix erosion (Panyam et al., 2003; Mittal et al., 2007). The physical state of the drug inside the NPs matrix might have an influence on the in vitro and in vivo release behavior of the drug. DSC indicated that ibuprofen mostly exists in a crystalline state inside all NPs irrespective of their polymer content. The last finding indicates that the main rate-limiting step affecting drug release will be the dissolution of drug crystals into the polymeric matrix followed by their diffusion out of the matrix into the release media. This finding also confirmed the role of NPs core wetting in enhancing drug dissolution and hence drug release. PEG2.5%-g-PLA NPs showed faster drug release rates compared to other formulations and this could be attributed to their PEG content that might led to rapide core wetting resulting in faster drug dissolution followed

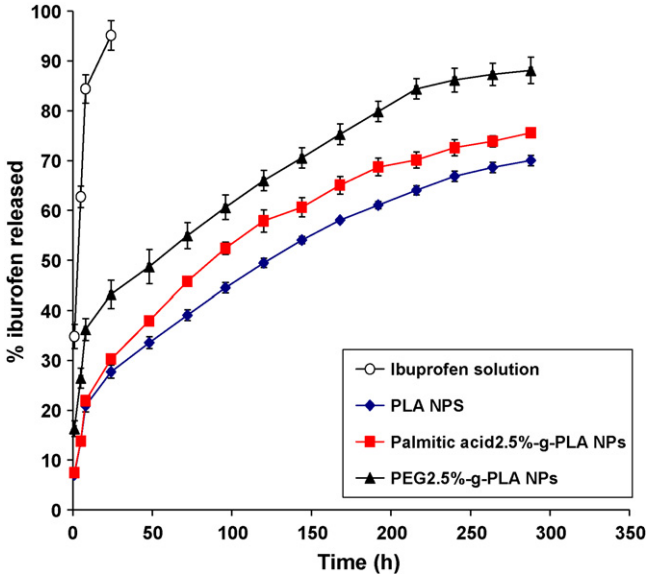

Fig. 7. Effect of PLA grafting on the in vitro release behavior of ibuprofen-loaded NPs; values are represented as mean ± S.D. of three independent experiments.

by its rapide diffusion and/or more enhancement of matrix erosion. On the other hand, palmitic acid2.5%-g-PLA NPs showed faster drug release compared to PLA NPs although the former is expected to be more hydrophobic and hence more interaction with drug will be favored. This is could be explained on the basis that PLA polymer had large molecular weight compared to palmitic acid2.5%-g-PLA polymer as shown before from GPC data (Table 1) and this might slow the process of matrix erosion (Peracchia et al., 1997). Erosion study showed that PEG2.5%-g-PLA NPs exhibited faster degradation rate (Fig. 6) than other NPs supporting the faster release behavior exhibited by those NPs. These results showed that the hydrophilicity of the matrix is one of the major factors that markedly influence its hydration and, in turn, the drug release profile (Sung et al., 1998; Sinha Roy and Rohera, 2002). It also should be mentioned that both erosion and release rates could be affected by the size of the particle tested. However, the small size differences between the three tested loaded batches (PLA, 162 ± 22.3 nm), (PEG-g-PLA, 135 ± 32.7 nm), and (palmitic acid-g-PLA, 183 ± 22.2 nm) might not be fully responsible for such big differences in both release and erosion.

4. Conclusion

NPs were fabricated using grafted copolymers of PLA with two grafted substances of different aqueous solubility. PEG2.5%-g-PLA NP and palmitic acid2.5%-g-PLA polymers were synthesized and fabricated into NPs. NPs were compared for the effect of the aqueous solubility of grafted substance of the polymer on their physicochemical properties. Mode of chain organization of each polymer was also investigated. Both AFM phase imaging and XPS studies showed the existence of PEG chains on the surface of PEG2.5%-g-PLA NPs. This resulted in rapide core wetting, faster degradation of the polymeric matrix and faster drug release from NPs. On the contrary, palmitic acid2.5%-g-PLA NPs showed the existence of palmitate chains embedded inside NPs core. This organization affected some major physicochemical properties of NPs. Our future work will focus on studying the cellular uptake of rhodamine encapsulated NPs made from different architectures. In brief, the aqueous solubility of grafted material over the polymer backbone is an important parameter controlling surface characteristics of NPs which in turn determine their physicochemical properties like % PVA adsorbed at the surface of NPs, zeta potential, thermal characteristic, NPs surface organization and drug release kinetics.

Acknowledgments

The work was supported in part by a grant of Fonds de la reserche en santé Québec (FRSQ) to Dr. Hildgen. The authors wish to thank Mme. Suzie poulin, research associate at École Polytechnique, University of Montreal for her help in the data analysis of the XPS experiments. Sherief Essa thanks the Ministry of Higher Education, Egypt for granting him a scholarship during his Ph.D.

References

Beletsi, A., Panagi, Z., Avgoustakis, K., 2005. Biodistribution properties of nanoparticles based on mixtures of PLGA with PLGA-PEG diblock copolymers. Int. J. Pharm. 298, 233–241.
Chorny, M., Fishbein, I., Danenberg, H.D., Golomb, G., 2002. Lipophilic drug loaded nanospheres prepared by nanoprecipitation: effect of formulation variables on size, drug recovery and release kinetics. J. Control. Release 83, 389–400.
Clapper, J.D., Skeie, J.M., Mullins, R.F., Guymon, C.A., 2007. Development and characterization of photopolymerizable biodegradable materials from PEG–PLA–PEG block macromonomers. Polymer 48, 6554–6564.
Donald, G., William, D., Randal, S., John, L., Willett, J.L., 2003. Mechanical and thermal properties of starch-filled poly(D,L-lactic acid)/poly(hydroxy ester ether) biodegradable blends. J. Appl. Polym. Sci. 88, 1775–1786.
Frank, A., Rath, S.K., Venkatraman, S.S., 2005. Controlled release from bioerodible polymers: effect of drug type and polymer composition. J. Control. Release 102, 333–344.
Gorner, T., Gref, R., Michenot, D., Sommer, F., Tran, M.N., Dellacherie, E., 1999. Lidocaine-loaded biodegradable nanospheres. I. Optimization of the drug incorporation into the polymer matrix. J. Control. Release 57, 259–268.
Govender, T., Riley, T., Ehtezazi, T., Garnett, M.C., Stolnik, S., Illum, L., Davis, S.S., 2000. Defining the drug incorporation properties of PLA–PEG nanoparticles. Int. J. Pharm. 199, 95–110.
Gref, R., Lück, M., Quellec, P., Marchand, M., Dellacherie, E., Harnisch, S., Blunk, T., Müller, R.H., 2000. 'Stealth' corona–core nanoparticles surface modified by polyethylene glycol (PEG): influences of the corona (PEG chain length and surface density) and of the core composition on phagocytic uptake and plasma protein adsorption. Colloids Surf. B: Biointerfaces 18, 301–313.
Heald, C.R., Stolnik, S., Kujawinski, K.S., De Matteis, C., Garnett, M.C., Illum, L., Davis, S.S., Purkiss, S.C., Barlow, R.J., Gellert, P.R., 2002. Poly(lactic acid)–poly(ethylene oxide) (PLA–PEG) nanoparticles: NMR studies of the central solidlike PLA core and the liquid PEG corona. Langmuir 18, 3669–3675.
Jacobsen, S., Fritz, H.G., 1999. Plasticizing polylactide—the effect of different plasticizers on the mechanical properties. Polym. Eng. Sci. 39, 1303–1310.
Jeong, Y.-I., Cheon, J.-B., Kim, S.-H., Nah, J.-W., Lee, Y.-M., Sung, Y.-K., Akaike, T., Cho, C.-S., 1998. Clonazepam release from core-shell type nanoparticles in vitro. J. Control. Release 51, 169–178.
Kim, Y., Pyun, J., Frechet, J.M.J., Hawker, C.J., Frank, C.W., 2005. The dramatic effect of architecture on the self-assembly of block copolymers at interfaces. Langmuir 21, 10444–10458.
Letchford, K., Burt, H., 2007. A review of the formation and classification of amphiphilic block copolymer nanoparticulate structures: micelles, nanospheres, nanocapsules and polymersomes. Eur. J. Pharm. Biopharm. 65, 259–269.
Magenheim, B., Levy, M.Y., Benita, S., 1993. A new in-vitro technique for the evaluation of drug-release profile from colloidal carriers—ultrafiltration technique at low-pressure. Int. J. Pharm. 94, 115–123.
Magonov, S.N., Elings, V., Whangbo, M.H., 1997. Phase imaging and stiffness in tapping-mode atomic force microscopy. Surf. Sci. 375, L385–L391.
Mittal, G., Sahana, D.K., Bhardwaj, V., Ravi Kumar, M.N.V., 2007. Estradiol loaded PLGA nanoparticles for oral administration: effect of polymer molecular weight and copolymer composition on release behavior in vitro and in vivo. J. Control. Release 119, 77–85.
Mohanraj, V.J., Chen, Y., 2007. Nanoparticles—A Review. Association of Crop Science, Uganda.
Nadeau, V., Leclair, G., Sant, S., Rabanel, J.-M., Quesnel, R., Hildgen, P., 2005. Synthesis of new versatile functionalized polyesters for biomedical applications. Polymer 46, 11263–11272.
Panyam, J., Dali, M.M., Sahoo, S.K., Ma, W., Chakravarthi, S.S., Amidon, G.L., Levy, R.J., Labhasetwar, V., 2003. Polymer degradation and in vitro release of a model protein from poly(D,L-lactide-co-glycolide) nano- and microparticles. J. Control. Release 92, 173–187.
Paredes, J.I., Gracia, M., Martínez-Alonso, A., Tascón, J.M.D., 2005. Nanoscale investigation of the structural and chemical changes induced by oxidation on carbon black surfaces: a scanning probe microscopy approach. J. Colloid Interface Sci. 288, 190–199.
Peracchia, M.T., Gref, R., Minamitake, Y., Domb, A., Lotan, N., Langer, R., 1997. PEG-coated nanospheres from amphiphilic diblock and multiblock copolymers: investigation of their drug encapsulation and release characteristics. J. Control. Release 46, 223–231.

Quesnel, R., Hildgen, P., 2005. Synthesis of PLA-b-PEG multiblock copolymers for stealth drug carrier preparation. Molecules 10, 98–104.
Raghavan, D., Gu, X., Nguyen, T., VanLandingham, M., Karim, A., 2000. Mapping polymer heterogeneity using atomic force microscopy phase imaging and nanoscale indentation. Macromolecules 33, 2573–2583.
Riley, T., Stolnik, S., Heald, C.R., Xiong, C.D., Garnett, M.C., Illum, L., Davis, S.S., Purkiss, S.C., Barlow, R.J., Gellert, P.R., 2001. Physicochemical evaluation of nanoparticles assembled from poly(lactic acid)–poly(ethylene glycol) (PLA–PEG) block copolymers as drug delivery vehicles. Langmuir 17, 3168–3174.
Sahoo, S.K., Panyam, J., Prabha, S., Labhasetwar, V., 2002. Residual polyvinyl alcohol associated with poly(D,L-lactide-co-glycolide) nanoparticles affects their physical properties and cellular uptake. J. Control. Release 82, 105–114.
Sant, S., Poulin, S., Hildgen, P., 2008. Effect of polymer architecture on surface properties, plasma protein adsorption, and cellular interactions of pegylated nanoparticles. J. Biomed. Mater. Res. Part A 87A, 885–895.
Scholes, P.D., Coombes, A.G.A., Illum, L., Davis, S.S., Watts, J.F., Ustariz, C., Vert, M., Davies, M.C., 1999. Detection and determination of surface levels of poloxamer and PVA surfactant on biodegradable nanospheres using SSIMS and XPS. J. Control. Release 59, 261–278.
Shakesheff, K.M., Evora, C., Soriano, I., Langer, R., 1997. The adsorption of poly(vinyl alcohol) to biodegradable microparticles studied by X-ray photoelectron spectroscopy (XPS). J. Colloid Interface Sci. 185, 538–547.
Sinha Roy, D., Rohera, B.D., 2002. Comparative evaluation of rate of hydration and matrix erosion of HEC and HPC and study of drug release from their matrices. Eur. J. Pharm. Sci. 16, 193–199.
Siparsky, G.L., Voorhees, K.J., Dorgan, J.R., Schilling, K., 1997. Water transport in polylactic acid (PLA), PLA/polycaprolactone copolymers, and PLA polyethylene glycol blends. J. Environ. Polym. Degrad. 5, 125–136.
Sung, K.C., Han, R.-Y., Hu, O.Y.P., Hsu, L.-R., 1998. Controlled release of nalbuphine prodrugs from biodegradable polymeric matrices: influence of prodrug hydrophilicity and polymer composition. Int. J. Pharm. 172, 17–25.
Vila, A., Gill, H., McCallion, O., Alonso, M.J., 2004. Transport of PLA–PEG particles across the nasal mucosa: effect of particle size and PEG coating density. J. Control. Release 98, 231–244.
von Burkersroda, F., Gref, R., Göpferich, A., 1997. Erosion of biodegradable block copolymers made of poly(D,L-lactic acid) and poly(ethylene glycol). Biomaterials 18, 1599–1607.
Wang, H., Djurisic, A.B., Chan, W.K., Xie, M.H., 2005. Factors affecting phase and height contrast of diblock copolymer PS-b-PEO thin films in dynamic force mode atomic force microscopy. Appl. Surf. Sci. 252, 1092–1100.
Zambaux, M.F., Bonneaux, F., Gref, R., Maincent, P., Dellacherie, E., Alonso, M.J., Labrude, P., Vigneron, C., 1998. Influence of experimental parameters on the characteristics of poly(lactic acid) nanoparticles prepared by a double emulsion method. J. Control. Release 50, 31–40.